The structure and paramagnetism of Ni_3Nb

1992 J. Phys.: Condens. Matter 4 2405

(http://iopscience.iop.org/0953-8984/4/10/007)

J. Phys.: Condens. Matter 4 (1992) 2405–2414. Printed in the UK

The structure and paramagnetism of Ni_3Nb

Tao Fang†, S J Kennedy‡, Lin Quan§ and T J Hicks†

† Department of Physics, Monash University, Clayton 3168, Australia

‡ Australian Institute of Nuclear Science and Engineering, Private Mailbag, Menai 2234, Australia

§ Institute of Physics Academia Sinica, PO Box 603, Beijing, People's Republic of China

Received 14 June 1991, in final form 22 October 1991

Abstract. A single crystal of Ni_3Nb has been investigated with x-ray diffraction to determine the structure, and with bulk magnetic measurements and neutron polarization analysis to characterize the enhanced paramagnetic behaviour. The structure has been confirmed to be ordered and orthorhombic, having the space group *Pmmn*, and with lattice constants $a = 5.114$ Å, $b = 4.244$ Å, and $c = 4.53$ Å. The magnetization results do not produce straight Arrott plots and attempts to fit the magnetization to a model with a Langevin function describing local moments, in addition to a band component, yield local moments that vary with temperature. The paramagnetic neutron scattering agrees with the measured static susceptibility in the small-scattering-vector limit suggesting that the energy width of the scattering is much less than the energy of the incident neutrons (6 meV). The scattering vector dependence of the paramagnetic scattering can be fitted by a Lorentzian that is consistent with a paramagnetic enhancement factor of 40–50 assuming predominant first-neighbour exchange.

1. Introduction

Among the paramagnetic metals with strong ferromagnetic enhancement which have been studied are Pd, Ni_3Ga, and Ni_3Al, the last of which is weakly ferromagnetic, but becomes paramagnetic with a small reduction of Ni content. These metals are characterized by a large initial susceptibility which reduces markedly at higher fields. Addition of a small concentration of atoms with a fixed moment normally produces giant moments in which the impurity polarises the surrounding susceptible matrix so that the giant moment entity consists largely of a long-ranged component in the matrix. Neutron diffraction measurements of the induced moment range can give some idea of the degree of enhancement of the matrix susceptibility (Hicks *et al* 1968, Ling and Hicks 1973).

Recent neutron diffraction measurements by Lonzarich *et al* (1989) add a new dimension to the investigation of these materials. By measuring the purely paramagnetic scattering from Ni_3Ga not only can an estimate of the range of the giant fluctuations be made but also their lifetime.

In this paper we describe a series of measurements on the enhanced paramagnet Ni_3Nb. This material is not cubic like the other nickel compounds Ni_3Ga and Ni_3Al but has an orthorhombic structure with two distinct Ni sites. As the structure had previously only been determined twice by x-ray powder diffraction with conflicting results, we first checked the structure with x-rays using part of our single crystal

before making magnetic and neutron paramagnetic scattering measurements. With these latter results we are able to determine an enhancement factor of 40–50 and to provide circumstantial evidence that the lifetime of the paramagnetic fluctuations is long. At the same time we were able to confirm the magnetic nature of the small angle scattering seen with neutron polarization analysis.

2. The specimen

The crystal of Ni_3Nb, with a nominal composition of 26.1 at% of Nb, was grown using a Bridgman method at the Institute of Iron & Steel of Beijing. The specimen is ~ 2.5 cm in diameter at the bigger end and about 2.5 cm in length in the usual Bridgman ingot shape with a volume of 9.798 cm^3 and a density of 8.463 g cm^{-3}. Grossiord and Turpin (1973) found that the growing direction is very nearly parallel to the [100] axis. Initial x-ray Laue diffraction photographs of the tip of this crystal showed that the [100] axis deviates $\sim 15°$ from the growing direction.

More detailed x-ray diffraction measurements described in the following section show that the specimen is single phase in the Ni_3Nb structure. Atomic absorption analysis was employed to measure the concentration of other 3d transition elements, and 10, 126, and 531 ppm of Mn, Co, and Fe were detected. The last of these is high and might be expected to have considerable effect on the magnetic properties, but as will be detailed later the magnetic properties cannot simply be explained by giant moments formed about the iron impurities.

3. Crystal structure

A small specimen was cut from the tip of the crystal for x-ray crystallographic measurements. The aim was a spherical specimen of diameter 0.25 mm but a rough ellipsoid of 0.5 mm $\times 0.25$ mm $\times 0.25$ mm was what could be achieved by spark erosion. Data was taken with an automatic four-circle diffractometer using Mo K_α radiation. 852 reflections were collected at room temperature.

The result confirmed that Ni_3Nb is ordered and orthorhombic, having the space group *Pmmn*, and with lattice constants $a = 5.114$ Å, $b = 4.244$ Å, and $c = 4.538$ Å. It is a centrosymmetric structure with 8 atoms per unit cell, and because b and c are similar it can be considered distorted tetragonal.

The diffraction intensities, after eliminating those affected by extinction, were corrected for attenuation using the measured dimensions and orientation of the crystal, and were refined to determine precisely the atomic positions. An R factor of 4.57% was attained. The atomic coordinates are given in table 1 and the structure of the unit cell is shown in figure 1. The structure consists of approximately straight chains of Ni(1) and Nb atoms along the a direction. Pairs of Ni(1) and Nb atoms are joined in figure 1 to emphasise the chains of these atoms. Between the chains of Ni(1) and Nb atoms are straight chains of Ni(2), offset along the a direction by $a/4$.

It can be seen from table 1 that the atom positions are very similar to the powder diffraction results of Ruhl *et al* (1967). Column 2 shows that by shifting the origin of our unit cell by $-\frac{1}{4}$, $+\frac{1}{4}$, 0, Ruhl *et al*'s coordinates can be reproduced apart from small differences in the z-coordinates of all atoms and in the x-coordinates of the Ni(2) atoms. The same cannot be said of the Debye–Scherrer results of Kaufmann *et al* (1969) who determined a tetragonal unit cell.

Table 1. Atomic coordinates of Ni_3Nb from the present single-crystal results and the powder-diffraction results of Ruhl *et al* (1967).

	Single-crystal data						Ruhl *et al*		
Pmmm	Origin at $\bar{1}$			Origin at 1/4, −1/4, 0 from $\bar{1}$					
Atom	x/a	y/b	z/c	x/a	y/b	z/c	x/a	y/b	c/z
Nb (2b)	1/4	3/4	0.6513	0		0.6513	0	0	0.667
	3/4	1/4	0.3487	1/2	1/2	0.3487	1/2	1/2	0.333
Ni(1) (2a)	1/4	1/4	0.3182	0	1/2	0.3182	0	1/2	0.333
	3/4	3/4	0.6818	1/2	0	0.6818	1/2	0	0.667
Ni(2) (4f)	−0.0006	1/4	0.8414	0.7494	1/2	0.8414	3/4	1/2	0.833
	0.0006	1/4	0.1586	0.7506	0	0.1586	3/4	0	0.167
	0.5006	1/4	0.8414	0.2506	1/2	0.8414	1/4	1/2	0.833
	0.4994	3/4	0.1586	0.2494	0	0.1586	1/4	0	0.167

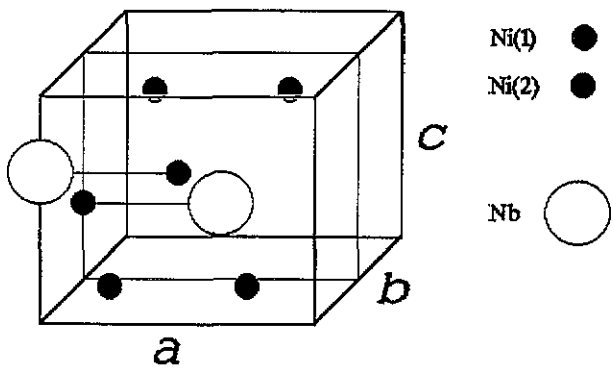

Figure 1. The structure of Ni_3Nb.

4. Magnetic measurements

The magnetic measurements were performed on an extraction magnetometer at the Institute of Physics in Beijing. At first sight (figure 2) the results are what might be expected for a ferromagnetically enhanced paramagnet. However when the results are plotted as an Arrott plot (the square of the magnetic moment versus the inverse susceptibility), rather than being straight lines, the isotherms are concave upwards. Similar Arrott plots have been obtained by Schinkel *et al* (1973) for Ni_3Ga and by Robbins and Claus (1971) for Ni_3Al. The effect is also seen in iron-doped Ni_3Al (Ling and Hicks 1973).

Because of the level of transition metal impurity detected in the Ni_3Nb sample the magnetization curves were fitted with an expression which included a Langevin term to describe the giant localized moments which may be induced in addition to electron band terms. The magnetization is written

$$M = CN\mu\left[\coth\left(\frac{\mu H}{k_B T}\right) - \frac{k_B T}{\mu H}\right] + \chi_0 H - aH^3 \qquad (1)$$

where C is the concentration of giant local moments μ, χ_0 is the initial band susceptibility, and a is the first correction coefficient to the band susceptibility. The fits

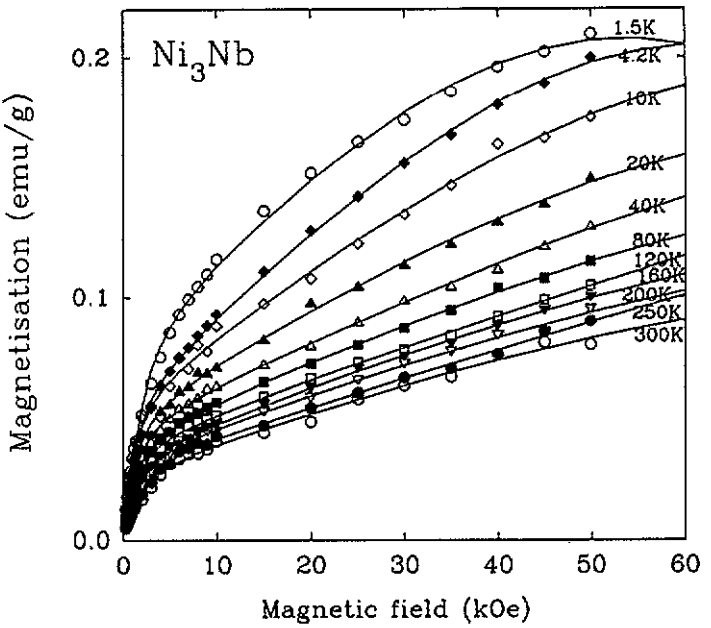

Figure 2. The variation of magnetization with applied field for Ni_3Nb at various temperatures.

of this expression to most of the isotherms are good and they are drawn as the full curves in figure 2. Exceptions are the isotherms for 250 K and 120 K where the error on the fitted value of a was large, and the 1.5 K isotherm where the sum of the squares of the residuals was rather larger than for the others. The unsatisfactory nature of this fit can also be seen in the downward turn in the fitted line at the highest field values.

Figure 3 shows the the values of C and μ obtained from the fits. The values for μ are surprisingly large but of the same order of magnitude as obtained by Robbins and Claus with a similar fit. More surprising is the variation of μ with temperature. If the moments were due to the transition metal impurities a value for μ independent of

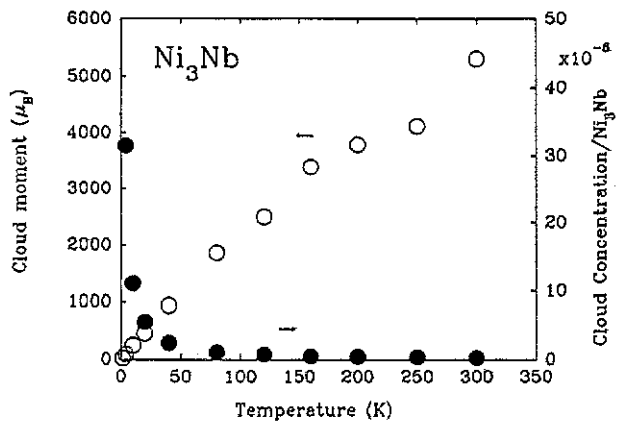

Figure 3. The variation of the fitted values of fixed moment concentration C (●) and moment μ (○) with temperature.

temperature would be expected. The order of magnitude of the moment associated with a transition metal impurity can be estimated from the work of Schalwijk *et al* (1971) by comparison with Ni_3Ga, Ni_3Al, and Pd. The susceptibility of Ni_3Nb is less than that of Pd at room temperature so that the giant moment induced by an Fe impurity is expected to be less than 10 μ_B. It is only at the lowest temperatures that the fitted moment approaches 10 μ_B. Robbins and Claus also found moments in excess of 1000 μ_B in their similar fit of the magnetization of Ni_3Al.

Figure 4 shows an Arrott plot of the fitted band component of the susceptibility. The fit constrains the isotherms to intersect the axis as straight lines. More significantly the isotherms have similar slopes and yield initial susceptibilities which increase with decrease of temperature. That is, superficially the Arrott plot looks close to what would be predicted by the Edwards and Wohlfarth (1968) RPA model of ferromagnetically enhanced band magnets. A plot (figure 5) of inverse initial susceptibility with temperature squared, however, reveals that this plot is not linear, contrary to the predictions of the Edwards and Wohlfarth model.

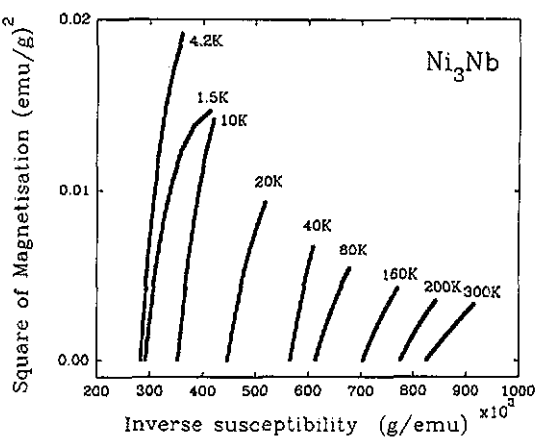

Figure 4. Arrott plot of the fitted band component of the magnetization.

5. Neutron scattering

In order to isolate the paramagnetic scattering a polarization analysis experiment was performed using the LONGPOL diffractometer-spectrometer (Cussen *et al* 1991). The instrument has recently been rebuilt and in several respects the experiment was less than ideal. Firstly, the paramagnetic scattering from Ni_3Nb was found to be concentrated at very small scattering angles. This meant that only two detectors could be used, and these had to be stopped down considerably to obtain the necessary angular resolution. Very little collimation of the incident beam was required as monochromation is by a dog-leg configuration which largely preserves the divergence of the in-pile collimator which is less than one degree. The ideal experiment would have been to alternate the polarization at the specimen position between vertical and along the elastic scattering vector. This would have given us the time-of-flight spectrum of the magnetic scattering at each angle, at least for small energy changes.

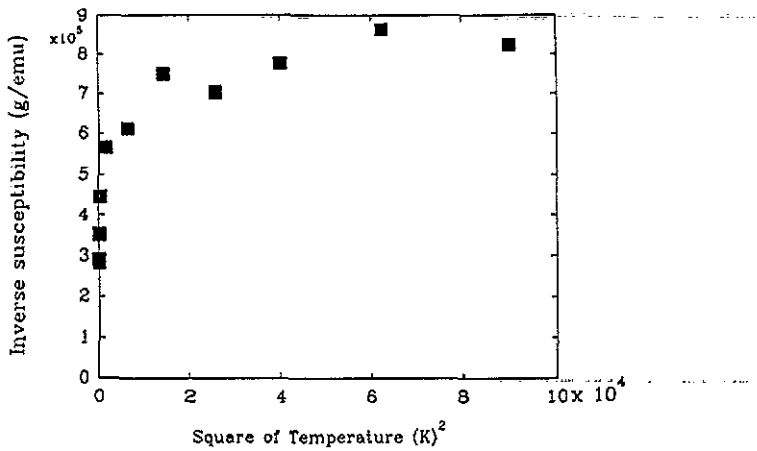

Figure 5. Plot of the inverse initial band susceptibility with temperature squared for comparison with the Edwards–Wohlfarth (1968) RPA band model.

Unfortunately we cannot yet reliably turn the neutron spins from vertical to horizontal because of relatively large fields in the vicinity. We therefore simply measured the spin-flip and non-spin-flip count rates with polarization vertical, so that half of the magnetic cross-section appears in the non-spin-flip, and half in the spin-flip count rate. Apart from the lack of time-of-flight information, this experiment yields twice the statistical error in the magnetic cross-section as would be obtained from an experiment in which the polarization is along the elastic scattering vector.

Because of the large air scattering at small angles very careful subtraction of the background was made. This was done with our usual technique of matching the attenuation of the specimen with a foil of indium. The specimen and indium were alternated with each monitor period (approx $3\frac{1}{2}$ minutes). The relative efficiency of the two detectors was measured by calibration with vanadium and by scanning the detectors through the main beam. The latter method was possible because of the extreme restriction of detector area necessary for angular resolution. Both methods gave the same relative efficiencies within error, but the latter was used because of its much higher accuracy. For absolute calibration we relied on the known incoherent cross-section of Ni in the specimen.

The total, nuclear, and magnetic count rates are shown in figure 6. The first four points from one detector have been adjusted upward by the measured relative calibration factor to be comparable with the last four points from the other detector. The total count rate from the specimen increases towards small scattering vectors. This is reflected in the magnetic count rate while the nuclear count rate is relatively constant.

To obtain a clearer view of the magnetic cross-section we made the assumption that the nuclear scattering is κ-independent, as would be expected if it were due merely to the nickel incoherent cross-section. The average nuclear count rate was subtracted from the much more accurate total count rate to give a more accurate estimate of the magnetic intensity. At the same time the nuclear intensity, corrected for 17% multiple scattering, was used to put the magnetic intensity on an absolute cross-section basis. These results are shown in figure 7 and the errors shown are total statistical errors only. Also shown are estimates of the $\kappa = 0$ cross-section calculated

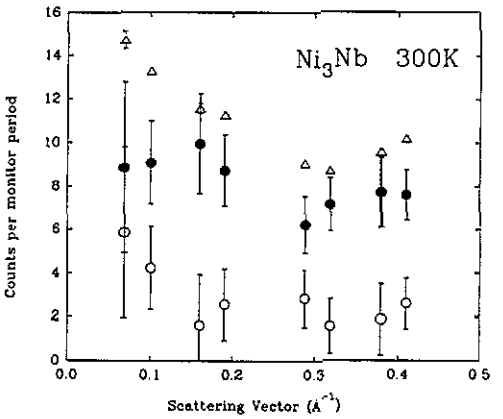

Figure 6. Raw total △, nuclear ●, and magnetic ○, count rates at 300 K corrected for background and attenuation.

from the bulk susceptibility. The lower estimate, indicated by an open circle, is simply M/H for the lowest measuring field of 233 Oe at 300 K. The upper estimate, indicated by an open square, is the $H = 0$ value of the susceptibility from the fit in the previous section. This calculation was done using the quasi-elastic approximation

$$\frac{d\sigma}{d\Omega} = 2\left(\frac{e\gamma}{\hbar C}\right)^2 \chi(\kappa) k_B T \tag{2}$$

where if the susceptibility, $\chi(\kappa)$, is in emu per formula unit, the cross-section is also per formula unit. The neutron measurements were done in a vertical field of about 200 Oe which means that fluctuations of magnetization in the vertical and horizontal directions see different fields, ~ 200 Oe and 0 Oe respectively. Therefore, perhaps a better estimate of the $\kappa = 0$ cross-section would be the average of the two estimates, in acknowledgment of the experimental situation in which two different susceptibilitites orthogonal to the scattering vector are being measured.

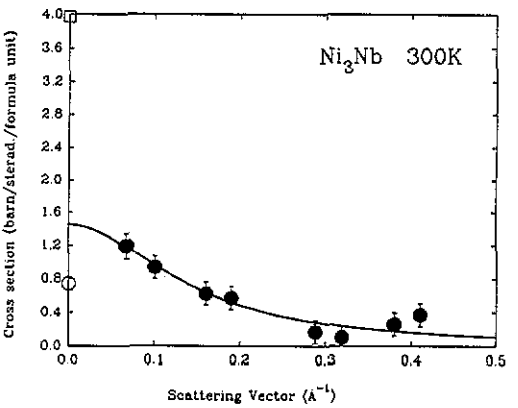

Figure 7. The magnetic crossection at 300 K obtained by assuming that the nuclear cross-section is independent of scattering vector at its average value. The calibration is with respect to the nuclear cross-section after correction for 17% multiple scattering.

In mean-field theory the wavevector-dependent susceptibility is given by

$$\chi(\kappa) = \frac{\chi_0}{1 - I(\kappa)\chi_0}. \tag{3}$$

This can be used to obtain an estimate of the the enhancement factor from the variation of cross-section with scattering vector. The wavevector-dependent exchange interaction is given by

$$I(\kappa) = \sum_R \mathcal{I}(R)e^{i\kappa \cdot R}. \tag{4}$$

If we assume that the exchange is predominantly with the closest nickel (Hicks 1977, 1980) and that this is approximately the same for all the atoms irrespective of whether they are Ni(1) or Ni(2), we have

$$I(\kappa) = \mathcal{I}(r)z(1 - \tfrac{1}{6}r^2\kappa^2) \tag{5}$$

for small κ and a spherical or cubically symmetric environment, and where r is the z closest neighbours approximate distance. The Ni_3Nb structure is not cubic, and what might be regarded as closest neigbours range in distance from each other from 2.56 Å to 2.63 Å. Nevertheless the structure is close enough to cubic and the neighbours close enough to being at the same distance to be useful for this rough estimate. We then obtain for the wavevector-dependent susceptibility

$$\chi(\kappa) = \frac{\chi_0}{(1 - z\mathcal{I}(r)\chi_0) + \frac{1}{6}z\mathcal{I}(r)\chi_0 r^2\kappa^2} \tag{6}$$

which is the expression fitted to the results in figure 7. Using $r = 2.59$ Å we find the enhancement factor $1/(1 - z\mathcal{I}(r)\chi_0) = 46.46$.

6. Discussion

At first sight the level of iron impurities appears to be so high as to mask any intrinsic magnetic behaviour of this material. This may indeed be true at low temperatures where the Curie-like susceptibility of the giant moments expected to be induced by the iron impurities would be large. But at high temperatures a generous estimate of the Curie susceptibility from giant moments ($20\mu_B$) yields no more than about 4% of the measured susceptibility. This point of view is further reinforced by non-Curie behaviour of the magnetization with field and temperature. Attempts to constrain the fixed moment value at 300 K to $20\mu_B$ yielded a much worse fit to the variation of moment with field, with a χ^2 value almost 100 times larger than the free fit. Attempts to start the the parameters well away from their best values, in particular starting the moment at low values, only saw the parameters move relentlessly to the same best values irrespective of the starting point, although considerable interdependence was observed in the movement of moment and concentration values.

The original reason for analysing the dependence of magnetization on field in terms of Langevin plus band paramagnetism, was because the Arrott plots are not straight even at the higher fields. It can be seen that the Langevin part of the

paramagnetic susceptibility is unlikely to be due to impurities and that the band part of the susceptibility does not conform to the Edwards–Wohlfarth (1968) analysis, at least in the variation of the inverse of the initial susceptibility with temperature. Moreover the temperature variation of the localized moment from the Langevin part of the susceptibility is quite strange and has no easy explanation except that if the fluctuations were large and also slow they might acquire statistics of their own, much like those that lead to the Langevin expression, but with a temperature dependence also a function of their band origin. The neutron cross-section, positively identified as magnetic using polarization analysis, is due to magnetic fluctuations which are long-ranged. The Lorentzian fit (figure 7) to the cross-section has a half-width at half maximum of 0.14 $Å^{-1}$ which is similar to that for Ni_3Ga (Lonzarich *et al* 1989). Comparison of the cross-section extrapolated to $\kappa = 0$ with the estimates of the susceptibility indicate that the quasi-elastic approximation for the calculation of the cross-section from the susceptibility is probably valid. This means that the inelasticity is much less than the thermal energy (25 meV) and the energy of the incident neutrons (6 meV). This is comparable to Ni_3Ga where the width of the central diffusive peak is about 0.5 meV or a relaxation time of about 5×10^{-11} s. These then are relatively slow and long-ranged fluctuations.

It may be worth investigating the enhancement of non-linear paramagnetic systems to see whether this offers some explanation for the behaviour of Ni_3Nb. Some saturation of the non-enhanced susceptibility would put more curvature into the variation of enhanced magnetization with field, possibly as we have observed. The fluctuations of moment in real space would no longer be of the Yukawa form but would be less enhanced in regions of large moment fluctuation so that large fluctuations would be longer-ranged. In that way the neutron cross-section may be more representative of the smaller fluctuations because the cross-section from the smaller number of large fluctuations would be limited to small scattering vectors.

7. Conclusion

The structure of Ni_3Nb has been confirmed to be ordered and orthorhombic, having the space group *Pmmn*, and with lattice constants $a = 5.114$ Å, $b = 4.244$ Å, and $c = 4.538$ Å. The magnetization results do not produce straight Arrott plots and attempts to fit the magnetization to a model with a Langevin function describing local moments in addition to a band component yield local moments which vary with temperature. The paramagnetic neutron scattering agrees with the measured static susceptibility in the small scattering-vector limit suggesting that the energy width of the scattering is much less than the energy of the incident neutrons (6 meV). The scattering-vector dependence of the paramagnetic scattering can be fitted by a Lorentzian which is consistent with an paramagnetic enhancement factor of 40–50 assuming predominant first-neighbour exchange.

Acknowledgments

The research was performed with financial assistance from the Australian Research Council and the Australian Institute of Nuclear Science and Engineering. LQ visited Australia for a short stay with assistance from the Chinese and Australian Academies of Science, and TF held a Monash University Postgraduate Award.

References

Cussen L D, Osborn J C, Gibbs P and Hicks, T J 1991 *Nucl. Instrum. Methods* at press
Edwards D M and Wohlfarth E P 1968 *Proc. R. Soc.* A **303** 127–3 7
Grossiord C and Turpin M 1973 *Metall. Trans.* **4** 1415–6
Hicks T J 1977 *J. Phys. F: Met. Phys.* **7** 481
—— 1980 *J. Phys. F: Met. Phys.* **10** 879
Hicks T J, Holden T M and Low G G 1968 *J. Phys. C: Solid State Phys.* **1** 528
Kaufman A, Hoffman N J and Lipson H 1969 *Scr. Metall.* **3** 715–20
Ling P C and Hicks T J 1973 *J. Phys. F: Met. Phys.* **3** 125–31
Lonzarich G G, Bernhoeft N R and Paul D McK 1989 *Physica* B **156–157** 699–705
Robbins C G and Claus H 1971 *Magnetism and Magnetic Materials (AIP Conf. Proc.No 5)* ed C D Graham and J J Rhyne pp 527–31
Ruhl R C, Giessen B C, Cohen M and Grant N J 1967 *J. Less-Common Metals* **13** 611–8
Schalwijk M S, Brommer P E, Cock G J and Schinkel C J 1971 *J. Physique Coll.* **32** 997–8
Schinkel C J, de Boer F R and de Hon B 1973 *J. Phys. F: Met. Phys.* **3** 1463–70